Proteomic Analysis for the Diagnosis of Fibrinogen Aα-Chain Amyloidosis

Graham W. Taylor[1], Janet A. Gilbertson[1], Rabya Sayed[1,2], Angel Blanco[1], Nigel B. Rendell[1], Dorota Rowczenio[1], Tamer Rezk[1,2], P. Patrizia Mangione[1], Diana Canetti[1], Paul Bass[2], Philip N. Hawkins[1] and Julian D. Gillmore[1,2]

[1]National Amyloidosis Centre and Wolfson Drug Discovery Unit, Centre for Amyloidosis and Acute Phase Proteins, University College London, London, UK; and [2]Centre for Nephrology, Division of Medicine, Royal Free Campus, University College London, London, UK

Introduction: Hereditary fibrinogen Aα-chain (AFib) amyloidosis is a relatively uncommon renal disease associated with a small number of pathogenic fibrinogen Aα (FibA) variants; wild-type FibA normally does not result in amyloid deposition. Proteomics is now routinely used to identify the amyloid type in clinical samples, and we report here our algorithm for identification of FibA in amyloid.

Methods: Proteomics data from 1001 Congo red–positive patient samples were examined using the Mascot search engine to interrogate the Swiss-Prot database and generate protein identity scores. An algorithm was applied to identify FibA as the amyloid protein based on Mascot scores. FibA variants were identified by appending the known amyloidogenic variant sequences to the Swiss-Prot database.

Results: AFib amyloid was identified by proteomics in 64 renal samples based on the Mascot scores relative to other amyloid proteins, the presence of a pathogenic variant, and coverage of the p.449-621 sequence. Contamination by blood could be excluded from a comparison of the FibA score with that of the fibrinogen β and γ chains. The proteomics results were consistent with the clinical diagnosis. Four additional renal samples did not fulfill all the criteria using the algorithm but were adjudged as AFib amyloid based on a full assessment of the clinical and biochemical results.

Conclusion: AFib amyloid can be identified reliably in glomerular amyloid by proteomics using a score-based algorithm. Proteomics data should be used as a guide to AFib diagnosis, with the results considered together with all available clinical and laboratory information.

A myloid, an extracellular accumulation of misfolded, fibrillary insoluble protein, is diagnosed on the basis of its pathognomonic histologic appearance, notably apple-green birefringence when stained with Congo red and viewed under crossed polarized light.[1,2] More than 30 different proteins can generate amyloid fibrils *in vivo,* and these individual proteins form the basis of the classification of amyloidosis. The natural history, prognosis, and management of amyloidosis is dependent on the precursor protein from which the amyloid fibrils are derived (i.e., the amyloid type), which therefore needs to be identified in every patient

presenting with the disease. Renal amyloid usually manifests with proteinuria and/or chronic kidney disease and is the cause of approximately 1% of end-stage kidney disease in the Western world.[3] Amyloid deposits in the kidney may arise from immunoglobulin light chains, amyloid A, FibA,[4] apolipoproteins A-I, A-II, A-IV, C2, and C3,[5–9] lysozyme,[10] transthyretin,[11] and leukocyte chemotactic factor 2.[12] AFib amyloidosis accounts for <5% of the patients with renal amyloidosis attending our clinic. Autosomal-dominant AFib amyloidosis, first identified in 1993 in a Peruvian family,[4] is the most common form of hereditary renal amyloidosis in the United Kingdom and Europe[13,14] and is associated with more than 14 different mutations of the fibrinogen A α-chain gene (FGA), which is located on chromosome 4 and has 6 exons.[13,15] These mutations are either single nucleotide substitutions that encode the variants p.E545V, p.E545, p.E543K, p.E559V, p.P571H, p.R573L, p.G574F, and p.T557K or frameshift mutations that result in peptides containing

Correspondence: Julian D. Gillmore, National Amyloidosis Centre, Division of Medicine, Royal Free Campus, University College London, Rowland Hill Street, London NW3 2PF, UK. E-mail: j.gillmore@ucl.ac.uk

the C-terminal sequence VLITLG.[16] The known pathogenic frameshift variants encode p.G538Efs*30, p.F540Lfs*28, p.F540Sfs*27, p.V541Afs*27, p.E543Efs*25, and p.T544T*fs24. Three nonamyloidogenic fibrinogen Aα-chain variants also have been described: p.G538R, p.G538E, and p.R573H.[15] By far the most frequently identified amyloidogenic variant worldwide is p.E545V.[13] Studies on *ex vivo* amyloid deposits from patients with AFib amyloidosis have shown that the amyloid fibril protein is associated with the C-terminus of fibrinogen Aα-chain and that only variant fibrinogen Aα chain and not wild-type fibrinogen Aα chain is incorporated into the amyloid.[4] Indeed, AFib amyloidosis has never been reported in the absence of an FGA mutation.

Immunohistochemistry (IHC) is commonly used for the identification of amyloid type; however, it fails to unambiguously determine the amyloid type in up to 30% of cases of systemic amyloidosis because of a combination of high background staining, lack of epitope specificity, and/or epitope masking.[17,18] Although AFib amyloid has a characteristic morphologic appearance on renal histology with isolated and often extensive glomerular infiltration, up to 10% of cases fail to stain immunohistochemically with antibodies against AFib.[13] Further, a similar structure occasionally can occur in light chain amyloidosis. Therefore, a proportion of cases of AFib amyloidosis currently are diagnosed on the basis of amyloid with typical renal morphology in the absence of specific IHC staining, in conjunction with the presence of a pathogenic FGA mutation on direct DNA sequencing, with the diagnosis sometimes further supported by a family history of the disease and/or a typical disease course.[13] More recently, proteomic analysis of amyloidotic tissue, a technique pioneered by the Mayo Clinic,[19–23] is now used in certain specialist amyloidosis centers to identify the amyloid fibril protein, complementing the diagnostic value of histology, IHC, and related techniques.[24–27]

We previously reported the identification of several novel variants of the AFib protein that are associated with renal amyloidosis.[13,28] Identification initially was made using gene analysis, with confirmation by immunohistochemistry and/or proteomics. Here, we sought to determine whether AFib amyloidosis could be diagnosed reliably by proteomic analysis using a simple algorithm to identify the specific variant amyloidogenic peptide and whether the issue of false positives through blood contamination of amyloid tissue can be avoided.

METHODS

Patients' Samples

This report covers patient data on 1001 Congo red–positive clinical samples obtained either as part of

standard clinical practice at the National Amyloidosis Centre or received from other hospitals requesting immunohistochemical and proteomics examination. Since early 2016, all clinical, biochemical, and proteomics data have been included within a single database at our center. A further 52 samples of pre-2016 patients with AFib were manually added to the database to increase the proportion of AFib cases in the current sample set. All samples had been identified as AFib amyloid at our weekly clinical proteomic meeting based on glomerular morphology and genetic and proteomics analysis. To obtain proteomics control data from fibrin, a sample of whole blood was collected from a healthy volunteer and was allowed to clot naturally. A small portion of the clot was formalin-fixed, embedded in paraffin, and treated as a normal sample.

All patients were managed in accordance with the Declaration of Helsinki, and informed consent for use of material and publication of data was obtained. The study was approved by the Royal Free Hospital Ethics Committee.

Sample Collection and Digestion

Sections were cut from a single sample block for Congo red and IHC staining as previously reported.[17,26] Amyloid was identified by presence of apple green birefringence when viewed under crossed polarized light. Congo red–positive material (a 6-μm section) was microdissected using a Leica LMD7 laser capture microscope (Leica Microsystems, Wetzlar, Germany) and collected into 0.5-ml microcentrifuge tubes (Eppendorf, Stevenage, UK) containing 35-μl tris(hydroxymethyl)-aminomethane/ethylenediamine tetraacetic acid/0.002% Zwittergent buffer (Sigma-Aldrich, St. Louis, MO). Samples were heated at 98 °C for 90 minutes with occasional vortexing. Following 60 minutes of sonication in a water bath, samples were digested with 30-ng trypsin (Promega Corporation, Madison, WI) overnight followed by treatment with dithiothreitol (50 μg) at 99 °C for 5 minutes. Water was removed under vacuum and the samples were redissolved in 0.1% aqueous trifluoroacetic acid (Fisher Scientific, Loughborough, UK) for proteomics analysis.[27,29,30]

Protein Identification

Proteomics analysis was undertaken on either a Thermo Scientific Orbitrap Velos hybrid Ion Trap-Orbitrap Mass Spectrometer (Thermo Fisher Scientific GmbH, Bremen, Germany) coupled to a Waters nanoAcquity UPLC system (Waters Corp., Milford, MA)[29] or, more recently, on a Thermo Scientific Q-Exactive Plus instrument connected to an Ultimate 3000 nanoLC system using a Thermo Easy-spray Acclaim PepMap column (75 μm × 15 cm, 3 μm/100 Å packing). Elution was undertaken at 300 nl/min with a 30-min linear gradient

of acetonitrile:water:formic acid (5:95:0.1–60:40:0.1 v/v/v). Optima LCMS-grade water, formic acid, and trifluoroacetic acid were obtained from Fisher Scientific, UK. Chromasolv LC-MS acetonitrile was obtained from Honeywell Research Chemicals, Riedel-de Haën, Germany. The new instrument was validated against a panel of clinical samples. Raw mass spectra data files initially were queried by Mascot (Matrix Science, London, UK) using the Swiss-Prot human protein database. Amyloid was identified by the presence of 2 or more of the signature proteins[22] proteins: apolipoprotein E, apolipoprotein A-IV, and serum amyloid P component. Following the initial database search, a modified database containing 13 known amyloidogenic variant fibrinogen Aα chain peptide sequences was appended to Swiss-Prot and the data were reanalyzed via this new database. The additional database included the most common amyloidogenic variant, p.E545V, together with the other known amyloidogenic variants—p.E543K, p.E545K, p.T557K, p.E559V, p.P571H, p.R573L, p.G574F, p.G538Efs*30, and p.F540Lfs*28—and the nonamyloidogenic variants p.G538R, p.G538E, and p.R573H. A generic 3n+1 nucleotide deletion frameshift protein p.36-527 containing the C-terminal peptide VLITLG also was included in the database. Data were interpreted by a panel of operators with extensive experience in amyloid proteomics, initially in the absence of clinical details. The presence of amyloid is accepted for Congo red–positive material when 2 out of 3 signature proteins (ApoE, ApoA4, or serum amyloid P component) are present, each with a minimum Mascot score of 20 and 1 unique significant peptide (in cases where Congo red staining is equivocal or absent, the threshold is increased to a minimum Mascot score of 50 and 1 unique significant peptide). The minimum score for all other proteins is set at 80 with 2 unique peptides. The top scoring amyloidogenic protein normally is used to type the tissue, except when ApoA1 or ApoA4 may be implicated or when more than one potential amyloidogenic protein has been identified with a similar score. In these cases, a more detailed examination of the tissue type, clinical presentation, and biochemistry is required. When there are fewer than 5 proteins in total (excluding keratins and hemoglobin), the sample may be declared inadequate.

Polymerase Chain Reaction and Direct Sequencing of FGA

Genomic DNA was extracted from whole blood treated with ethylenediamine tetraacetic acid, as previously described.[31] A 707 base pair fragment of exon 5 of FGA was amplified by polymerase chain reaction assay and analyzed by automated sequencing. Polymerase chain reaction was carried out with Ready To Go tubes (Amersham Pharmacia Biotech, Amersham, Buckinghamshire, UK) using the solutions and cycling conditions previously described. Polymerase chain reaction products were purified with a QIAquick polymerase chain reaction purification kit (Qiagen, Hilden, Germany) and sequenced with the Big Dye Terminator v3.1 Cycle Sequencing Kit (Applied Biosystems, Foster City, CA) according to the kit manufacturer's protocols. The FGA gene sequence was analyzed on the Applied Biosystems 3130xl Genetic Analyzer using Applied Biosystems Sequencing Analysis Software version 5.4.24.[28]

RESULTS

The current study was undertaken to evaluate a proteomics algorithm designed to identify AFib as the amyloid type in the presence of blood contamination. The data were extracted from the National Amyloidosis Centre database, which since 2016 has been integrated with our proteomics database. Proteomics data were analyzed using the Mascot search engine (www.matrixscience.com) to interrogate the human Swiss-Prot database. Mascot, together with other commonly used proteomics engines, uses a probability-based algorithm to generate an identity score for each protein based on the quality and abundance of individual peptide mass spectra. A protein's Mascot score is derived from the number of total, unique, and significant peptides identified by the program; similar data, but lacking an overall protein summary score, often are reported using Scaffold software (Proteome Software, Portland, OR).[20,32] A full proteomics dataset is available in Supplementary Table S1.

The proportion of patients with AFib amyloidosis among those referred to the UK National Amyloidosis Centre with renal amyloidosis is ∼5%. To ensure development and testing of a robust diagnostic algorithm, the number of AFib amyloid samples (as well as other rare renal amyloid types with glomerular involvement, such as ALECT2 amyloid) was manually increased by incorporation into the new database of proteomics data from patients with AFib amyloidosis collected prior to 2016. After excluding duplicate and control samples, we examined 1001 Congo red–positive samples, of which 240 were renal and 761 were from other tissues; amyloid signature proteins were identified in 198 and 632 samples, respectively (Table 1). Because AFib amyloidosis is predominantly a renal disease, we used the identification of renal FibA as a preliminary diagnostic indicator when developing the algorithm.

AFib was identified by the Mascot search engine in 391 samples (of which 35% were renal). The frequency

Table 1. Sample selection based on the criteria adopted for the identification of fibrinogen Aα as the amyloid protein

Samples	Renal	Nonrenal	Total
All (Congo red–positive)	240	761	1001
Amyloid signature (at least 2/3 of ApoA-IV, ApoE, and SAP)	198	632	830
FibA identified	137	254	391
FibA score >80, 2	99	95	194
FibA score > (Bβ + γ)	84	30	114
FibA top score	68	10	78
FibA top score + FibA > (Bβ + γ)	68	6	74
FibA top score + FibA > (Bβ + γ) + amyloid signature	67	4	71
FibA top score + FibA > (Bβ + γ) + amyloid signature + variant	64	1	65
Variant present	68	1[a]	69
Likely AFib by proteomics: variant present but not either amyloid signature, top score, or FibA > (Bβ + γ)	4	0	3
IHC fibrinogen	44[b]	1[a]	45
AFib clinical diagnosis[c]	68	0	68

AFib, fibrinogen Aα-chain amyloid; ApoA-IV, apolipoprotein A-IV; ApoE, apolipoprotein E; FibA, fibrinogen Aα; IHC, immunohistochemistry; SAP, serum amyloid P.
[a]Soft tissue biopsy from patient with renal AFib amyloid (included in renal column).
[b]Includes all FibA proteomics-positive samples plus 8 labeled no-immunospecific staining; 16 samples were not analyzed because of insufficient material.
[c]See Table 2 for clinical details.

distribution of FibA scores for both renal and all samples is shown in Figure 1. Clearly, the presence of FibA alone is insufficient to determine FibA as the amyloid type. To reduce potential false identifications based on low scoring peptides, we set a minimum requirement for the Mascot score at ≥80 and at least 2
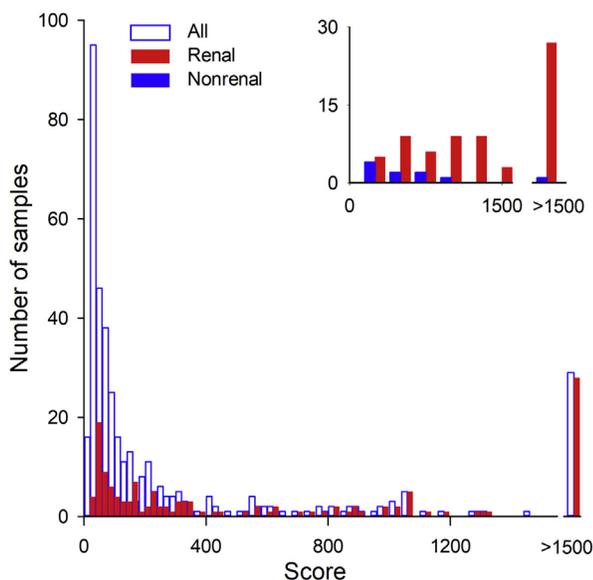
unique significant peptides, which excluded low-scoring proteins ($n = 197$) and reduced the positive FibA samples to 194 ($\sim$50% were renal). This number was further reduced to 78 samples (87% renal) as a result of the requirement for FibA to be the top-scoring amyloid fibril protein. The modified frequency distribution for top scoring FibA is shown in Figure 1 (inset) and demonstrates that higher scoring FibA is derived from renal rather than nonrenal samples.

The presence of blood in the tissues may result in a false-positive result, and thus the identification of FibA in amyloid tissues, even as the top-scoring protein, is on its own insufficient to make a diagnosis of AFib amyloidosis. In the current study, 85% of the samples contained hemoglobin A or B chains, with fibrinogen Bβ and γ chains present in $\sim$20% of all samples (Figure 2). Using hemoglobin as a marker of blood contamination and comparing scores against those of fibrinogen Aα, Bβ, and γ chains showed a qualitative difference between FibA and the other fibrinogen chains, which indicated that fibrinogen Bβ and γ chains were more dominant in samples contaminated by blood. To investigate whether AFib peptides could arise from the presence of blood within the tissue sample, a piece of normal clotted blood was formalin-fixed, embedded in paraffin, and then digested and analyzed in the same way as clinical tissues. Hemoglobin A and B chains were present with very high Mascot scores (7384 and 10,776, respectively). Wild-type fibrinogen A α
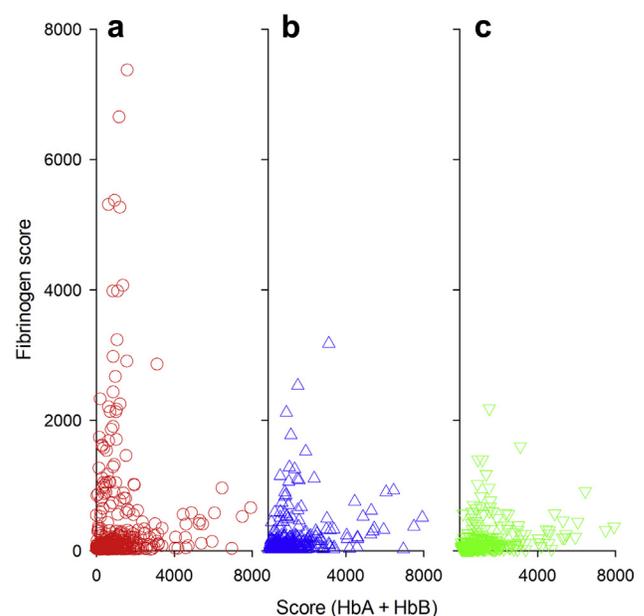

Figure 1. Frequency histogram showing the distribution of Mascot scores of significant protein identifications of fibrinogen Aα (FibA) in all samples (blue open bars, $n = 391$) and renal samples (red solid bars, $n = 137$). By requiring both a minimum acceptable score and FibA to be the top scoring amyloid protein, the number of FibA-positive samples is reduced to 78 (87% renal) and are associated with renal (red solid bars, inset) rather than nonrenal (blue solid bars, inset) samples.

Figure 2. The Mascot scores for fibrinogen Aα (a, red circles), Bβ (b, blue triangles), and γ (c, green triangles) chains plotted against the summed score for hemoglobins A and B (HbA and HbB) chains. There is a qualitative difference between FibA and the other groups.

chain was present (score 554) together with higher scores for fibrinogen Bβ and γ chains (640 and 490, respectively). Although probability scores are not quantitative, these data are consistent with the presence of similar amounts of the 3 fibrinogen chains in blood, as expected. This enabled us to modify our algorithm to include the requirement that the score of FibA be greater than the sum of scores of fibrinogens Bβ and γ (Figure 3). After further selecting for the samples in which FibA was the top-scoring amyloid protein, we were left with 71 samples (67 renal) that fulfilled the following requirements: FibA as the top-scoring amyloid fibril protein plus the score FibA > (Bβ + γ).

Interrogation of each of the 194 samples that were identified by a FibA Mascot score ≥80 and 2 unique significant FibA peptides, using a modified Swiss-Prot database containing the fibrinogen A α-chain variant peptide sequences, revealed the presence of a known pathogenic variant AFib peptide in 68 renal samples and 1 nonrenal (soft tissue) sample. All were associated with FibA as a top-scoring protein and the score of FibA > (Bβ + γ). The variant was p.E545V in 63 cases and p.E543K, p.E545K, p.P571H, p.571K, p.G538Efs*30, and p.F540Lfs*28 in 1 case each. Sequencing of exon 5 of the FGA gene was undertaken in all cases and confirmed the proteomics identification of the variant fibrinogen. The single
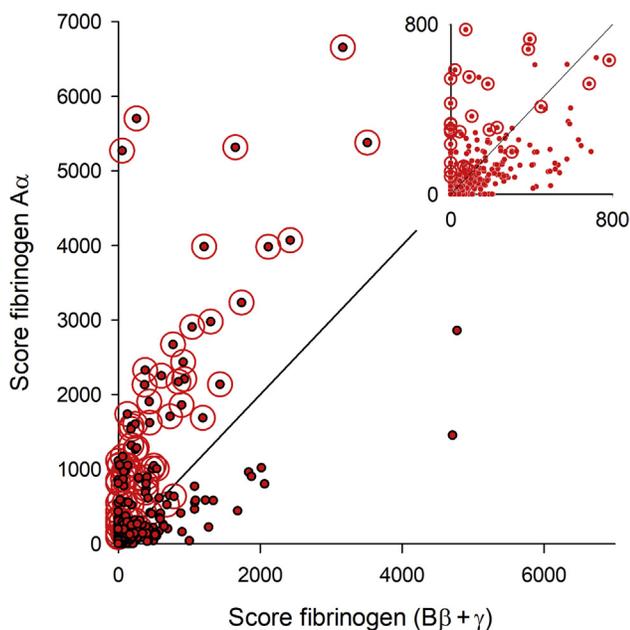
example of variant FibA detected in a nonrenal sample was from a soft tissue biopsy taken from a patient with AFib amyloidosis and where p.E545V FibA also had been identified by proteomics in renal tissue. No proteomics evidence for variant fibrinogens was observed in any of the other samples. Further, no FGA mutations were identified in those for which only wild-type fibrinogen had been identified in their microdissected glomerular sample. There were 3 samples in which 2 peptide variants, together with wild-type FibA, were identified by proteomics, although FGA sequencing indicated that only 1 variant was present. The quality of the raw mass spectra eliminated the possibility of misidentification of these apparent variant peptides. They were observed only when variant lysine was included at positions p.573 or p.575 in the database, generating a new in silico tryptic site. The peptides were C-terminal to the lysine and did not contain the variant residue, suggesting that they were indeed present, perhaps derived from wild-type FibA by postdeposition truncation, but were misidentified as tryptic peptides by the variant database search. We observed that coverage of the amyloidogenic FibA C-terminal fragment appeared to be substantially different between the 68 renal samples with AFib amyloid and all other FibA-positive samples. This is clearly shown in Figure 4, where the summed coverage at each residue is shown for the AFib amyloid samples compared with all other samples containing FibA. Because of the difference between groups at p.449, this was selected as the differentiation point between AFib samples. The median (interquartile range) percentage coverage of p.449-621 was for AFib amyloid and other samples, respectively (Figure 4); coverage of the remaining protein (p.20-448) was similar for both AFib and other groups at 5.7% (3.3–8.5) and 7.7% (4.3–10.5). Increased coverage of the p.449-621 region is a further indicator for the deposition of FibA in amyloid deposits. Although the difference in coverage is qualitatively observable, it was not considered suitable for quantitative analysis

Based on these data, we set the following criteria, all of which should be met, for the identification of AFib amyloid by proteomics: (i) amyloid on Congo red staining; (ii) presence of an amyloid signature (≥2 of 3 amyloid signature proteins: serum amyloid P, ApoE, or ApoA-IV); (iii) FibA identified with a minimum Mascot score of 80 and 2 unique significant peptides; (iv) FibA as the top-scoring amyloid protein; (v) the score of FibA greater than the sum of scores for fibrinogen Bβ + γ chains; and (vi) the presence of a pathogenic variant. A greater sequence

Figure 3. Comparison of individual fibrinogen Aα (FibA) Mascot scores with the sum of scores for fibrinogen (Fib)Bβ and γ chains in all 1001 Congo red–positive samples. Top scoring FibA (superimposed red open circles) is associated with samples where the score of FibA is greater than Fib(Bβ + γ). The line of equivalence for FibA/Fib(β + γ) scores is shown, together with an expanded scale figure (inset).
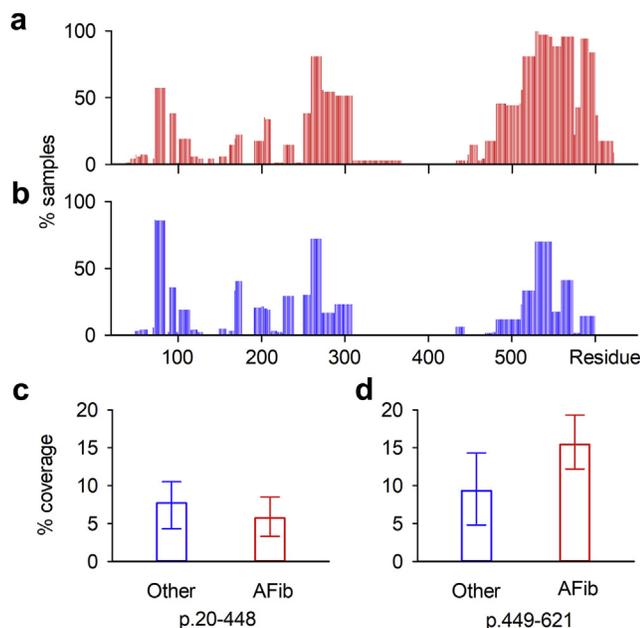
Figure 4. Protein coverage of fibrinogen Aα (FibA) for all samples with the minimum acceptable score is shown for samples from patients diagnosed with fibrinogen Aα-chain (AFib) amyloidosis (a, n = 68) and all other FibA-containing samples (b, n = 126). Data are normalized to the sample size. The median percentage coverage and interquartile ranges are shown for residues p.20-448 and p.449-621 for AFib and other samples in (c) and (d), respectively. These data are a guide to the difference in coverage; however, we do not believe that these data are amenable to statistical analysis.

coverage between p.449-621 was strongly associated with AFib amyloid. Based on our proteomics algorithm criteria, 64 renal samples and 1 nonrenal sample fulfilled all the criteria for AFib amyloidosis (Table 1, Figure 5).

IHC analysis was undertaken on 845 Congo red–positive samples, of which 45 were identified as AFib amyloid (including the single FibA–positive soft tissue sample). Other proteins identified included AA (27), λ (153), κ (36), LECT2 (12), and TTR (136), with no immunospecific staining mainly arising from κ/λ in 415 samples. Of the 65 samples identified as AFib amyloid by proteomics, 45 were diagnosed as AFib amyloid by IHC, 8 were recorded as no immunospecific staining, and the remainder were not analyzed by IHC because of the lack of sufficient available tissue.

A diagnosis of AFib amyloidosis, based on clinical presentation together with immunohistochemical, clinical biochemistry, and genetic analysis, was made in 68 cases (all renal, Table 2), including all of the 64 renal samples designated AFib amyloid by our algorithm. The remaining 4 clinical AFib cases were all positive for a pathogenic variant but were not diagnosed from the proteomics algorithm because 1 criterion was not achieved. One Congo red–positive sample

was defined as inadequate by proteomics but still showed a single amyloid signature protein together with a positive result for FibA. Another sample did not show FibA > (Bβ + γ) in the initial search, and in 2 samples either heavy chain or light chain κ were the top scoring proteins. In each case the clinical, morphologic, and laboratory data were consistent with AFib amyloid. Both the proteomics algorithm and clinical and biochemical parameters excluded a AFib amyloid in all other samples.

DISCUSSION

Diagnosis of hereditary AFib amyloidosis can be challenging because pathogenic FGA mutations are associated with variable disease penetrance such that there may be no family history of renal dysfunction in affected individuals.[13] IHC staining is not always successful, and the characteristic AFib amyloid renal biopsy morphology of isolated glomerular amyloid may occur, albeit rarely, in other amyloidoses. Proteomic analysis of Congo red–positive laser microdissected tissue samples, introduced by Dogan and colleagues at the Mayo Clinic,[19–23] is now used routinely in our center for the identification of amyloid deposits.[29,30,33] We use a single database search engine (Mascot) to identify proteins, although we note that others conjoin the results from multiple engines.[22,34,35] Although each of the major search engines can readily identify the major components present in a mixture, they may separately identify additional and different low-abundance peptides. Although this can be of value when analyzing large protein datasets,[36] it is perhaps of less importance for identifying a known amyloidogenic protein as a major component in laser-captured Congo red–positive tissue where the amyloid protein is concentrated and background impurities are reduced. Probability-based methods such as Mascot are not quantitative; however, more abundant proteins are normally associated with higher probability scores, which can be used as surrogate markers for protein amount.

Identification of more than one fibril protein by proteomic analysis of micro-dissected amyloid can result in ambiguity with respect to determining the amyloid type.[30] In the case of FibA, the protein can arise from small insoluble thrombi sealed within excised tissue samples that are placed directly into formalin-saline and typically is associated with the co-presence of fibrinogen Bβ and γ peptides on sample digestion. Further, extensive washing of fixed tissue before digestion often fails to eliminate thrombus-derived fibrinogen. In our sample set, >85% of samples contained hemoglobin and 20%
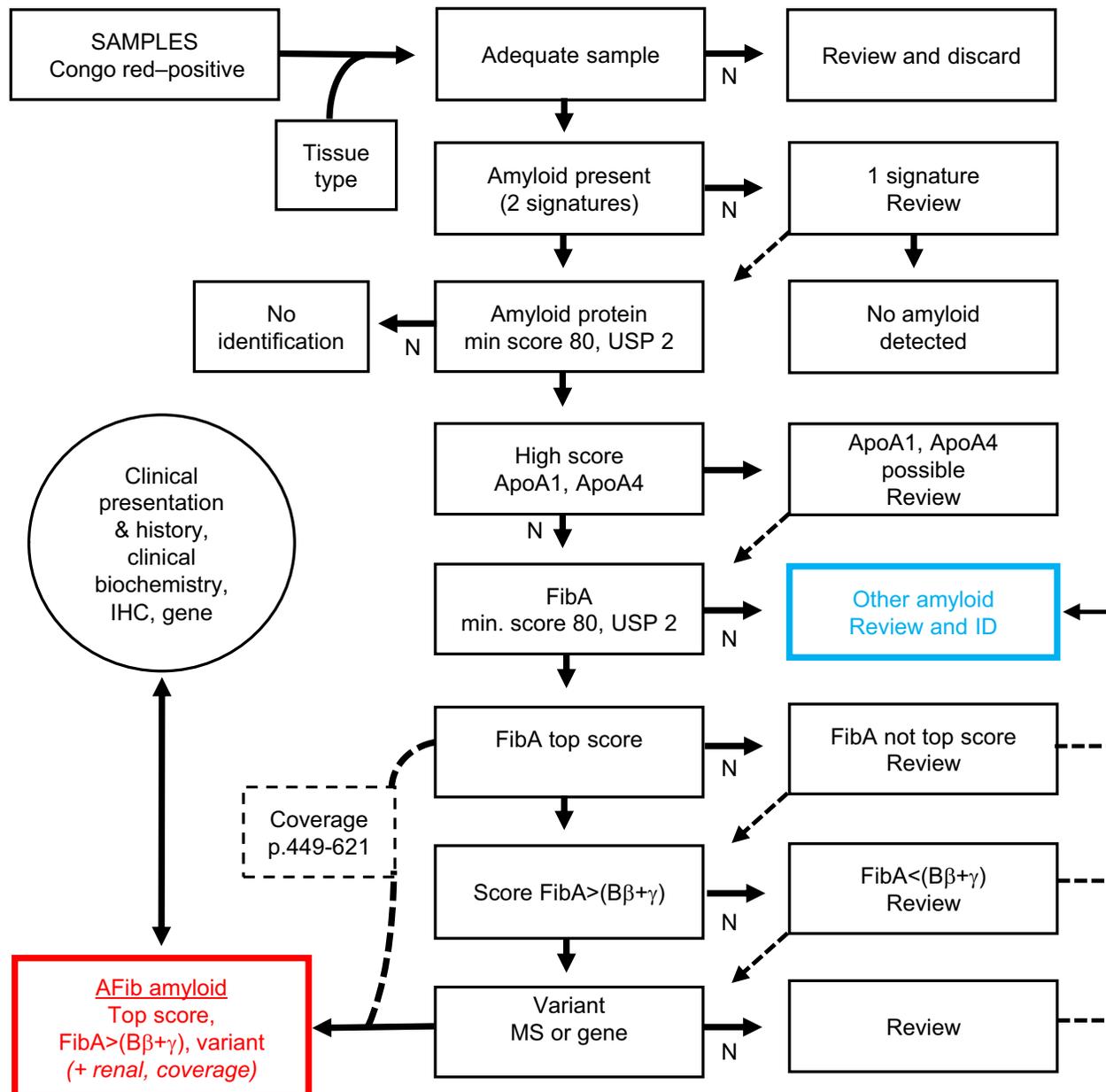
Figure 5. The proteomics algorithm for identifying fibrinogen Aα (FibA) as the amyloid protein. The algorithm is based on the Mascot score of amyloid and signature proteins together with the number of unique significant peptides (USPs) identified by the search engine. It is essential to apply the results of the proteomics algorithm in conjunction with clinical and laboratory data. Apo, apolipoprotein; ID, identification; IHC, immunohistochemistry; min, minimum; MS, mass spectrometric analysis.

contained fibrinogen Bβ and γ chains, consistent with blood contamination. By including a requirement for the score of FibA to be greater than the sum of scores for fibrinogens Bβ and γ, amyloid can be identified even in the presence of blood contamination. A high FibA residue coverage between p.449-621 was a further indicator of AFib amyloid, albeit nonspecific for the diagnosis. This is likely to reflect the fact that the amyloid is believed to be composed of a cleaved fragment of FibA containing this region.[4] This observation can be used as an additional guide to the possible presence of AFib amyloid.

The identification of a pathogenic variant by proteomics was central to the development of our diagnostic algorithm. Because wild-type AFib is not known to be amyloidogenic, the presence of a known amyloidogenic variant fibrinogen peptide or the generic frameshift protein containing the C-terminal peptide VLITLG in the specimen is diagnostic of AFib amyloidosis. Proteomics is sample type independent and, in principle, is ideally suited to variant analysis. In this study the variant in all 68 renal samples from AFib patients were identified, with findings corroborated in each case by DNA sequencing. The likely presence of truncated

Table 2. Summary of demographic or clinical characteristics of patients with fibrinogen Aα-chain amyloidosis

AFib amyloid diagnoses	
Total	68
Male	41
Female	27
Age at diagnosis, yr, median (range)	60 (7–84)
Congo red–positive, *n*	68
Immunohistochemistry	
Fibrinogen Aα–positive	44
No immunospecific staining	8
Not done	16
Kidney amyloid by SAP scintigraphy at diagnosis	
Yes	52
Not done	16
Supine systolic blood pressure at diagnosis, mm Hg, median (range)	147 (119–179)
Standing systolic blood pressure at diagnosis, mm Hg, median (range)	148 (117–191)
Serum creatinine at diagnosis, μmol/L, median (range)	226 (73–761)
Serum albumin at diagnosis, g/L, median (range)	31 (14–48)
24-h urinary protein loss at diagnosis, g, median (range)	6.2 (0.1–29.7)
eGFR at diagnosis, ml/min per 1.73 m^2, median (range)	22.5 (15–83)
Median time from diagnosis to ESRD by KM, mo, median	24
Time from diagnosis to dialysis among patients who reached ESRD, mo	
n	40
Median	15.4
Range	−160.4[a]–87.6
Time from diagnosis to kidney transplantation among patients who received a kidney transplant, mo	
n	17
Median	30.9
Range	−65.5[b]–112.7

AFib, fibrinogen Aα-chain; eGFR, estimated glomerular filtration rate; ESRD, end-stage renal disease; KM, Kaplan-Meier analysis; SAP, serum amyloid P.
[a]Commenced dialysis prior to diagnosis.
[b]Received kidney transplant prior to diagnosis.
No immunospecific staining is nondiagnostic of amyloid type.

FibA in some amyloid deposits explains the apparent identification of 2 separate variants in a some samples, which demonstrates the importance of discernment in the interpretation of search results, particularly when using modified or extended databases. The variant peptide approach of proteomics will not identify novel, previously unreported variants or those that form tryptic peptides, which are too small or large to generate good-quality spectra—hence the utility of the other proteomic data in generating a high index of suspicion of AFib amyloidosis that should prompt genetic testing.

The algorithm for proteomics diagnosis of AFib amyloid (Figure 5) is designed as a guide to diagnosis and should be used in conjunction with clinical and biochemical data. The model in our specialist center is to interpret proteomics data in the context of a weekly multidisciplinary meeting. We have set thresholds for FibA and other protein scores based on our extensive proteomics dataset coupled with our clinical and biochemical experience. Each sample in our database is individually reviewed by a team consisting of a senior clinician together with members of the biochemistry and proteomics groups. Sixty-eight patients from this data group were diagnosed with renal AFib amyloidosis. The algorithm was in agreement in 64 of 68 of these cases. Each of the remaining 4 patients with AFib was not diagnosed on the basis of the proteomics algorithm because of the failure of a single criterion, but each had a FibA variant, identified by both proteomics and genetic sequencing, and a characteristic clinical picture.

In conclusion, the diagnosis of AFib amyloidosis may be diagnosed confidently on the basis of the proteomics algorithm reported here, which takes into account the probability-based identity score of FibA compared with that of other potential amyloid proteins, the score relationship between the fibrinogens Aα, Bβ, and γ chains, coverage of the p.449-621 region, and the presence of an amyloidogenic FibA variant. A general amyloidosis diagnostic algorithm has been reported recently.[37] Although algorithms offer an objective approach to amyloid identification, we are of the firm opinion that proteomics results always should be examined in conjunction with clinical details together with the results of immunohistochemistry, genetic results, and clinical biochemistry.

AUTHOR CONTRIBUTIONS

JDG, GWT, and RS were responsible for conceiving the study, interpreting the results, and drafting the manuscript. JAG, DR, NBR, PPM, TR, DC, PB and PNH were responsible for data collection and interpretation of results, NBR and AB set up proteomics and clinical databases, respectively, and AB developed the protocols for data extraction from the databases. Authors were present at various times at the weekly clinical proteomics meetings where all data were reviewed.

SUPPLEMENTARY MATERIAL

Table S1. Proteomics data for each patient.

Supplementary material is linked to the online version of the paper at www.kireports.org.

REFERENCES

1. Puchtler H, Sweat F, Levine M. On the binding of Congo red by amyloid. *J Histochem Cytochem*. 1962;10:355–364.

2. Pepys MB. Amyloidosis. *Ann Rev Med*. 2006;57:223–241.

3. Fassbinder W, Brunner FP, Brynger H, et al. Combined report on regular dialysis and transplantation in Europe, XX, 1989. *Nephrol Dial Transplant*. 1991;6(suppl 1):5–35.

4. Benson MD, Liepnieks J, Uemichi T, et al. Hereditary renal amyloidosis associated with a mutant fibrinogen alpha-chain. *Nat Genet*. 1993;3:252–255.

5. Soutar AK, Hawkins PN, Vigushin DM, et al. Apolipoprotein AI mutation Arg-60 causes autosomal dominant amyloidosis. *Proc Natl Acad Sci U S A*. 1992;89:7389–7393.

6. Benson MD, Liepnieks JJ, Yazaki M, et al. A new human hereditary amyloidosis: the result of a stop-codon mutation in the apolipoprotein AII gene. *Genomics*. 2001;72:272–277.

7. Sethi S, Theis JD, Shiller SM, et al. Medullary amyloidosis associated with apolipoprotein A-IV deposition. *Kidney Int*. 2012;81:201–206.

8. Nasr SH, Dasari S, Hasadsri L, et al. Novel type of renal amyloidosis derived from apolipoprotein-CII. *J Am Soc Nephrol*. 2017;28:439–445.

9. Valleix S, Verona G, Jourde-Chiche N, et al. D25V apolipoprotein C-III variant causes dominant hereditary systemic amyloidosis and confers cardiovascular protective lipoprotein profile. *Nat Commun*. 2016;7:10353.

10. Pepys MB, Hawkins PN, Booth DR, et al. Human lysozyme gene mutations cause hereditary systemic amyloidosis. *Nature*. 1993;362:553–557.

11. Andersson R. Familial amyloidosis with polyneuropathy. A clinical study based on patients living in northern Sweden. *Acta Med Scand Suppl*. 1976;590:1–64.

12. Benson MD, James S, Scott K, et al. Leukocyte chemotactic factor 2: a novel renal amyloid protein. *Kidney Int*. 2008;74: 218–222.

13. Gillmore JD, Lachmann HJ, Rowczenio D, et al. Diagnosis, pathogenesis, treatment, and prognosis of hereditary fibrinogen A alpha-chain amyloidosis. *J Am Soc Nephrol*. 2009;20: 444–451.

14. Stangou AJ, Banner NR, Hendry BM, et al. Hereditary fibrinogen A alpha-chain amyloidosis: phenotypic characterization of a systemic disease and the role of liver transplantation. *Blood*. 2010;115:2998–3007.

15. Rowczenio DM, Noor I, Gillmore JD, et al. Online registry for mutations in hereditary amyloidosis including nomenclature recommendations. *Hum Mutat*. 2014;35:E2403–E2412.

16. Garnier C, Briki F, Nedelec B, et al. VLITL is a major cross-beta-sheet signal for fibrinogen Aalpha-chain frameshift variants. *Blood*. 2017;130:2799–2807.

17. Tennent GA, Cafferty KD, Pepys MB, et al. Congo red overlay immunohistochemistry aids classification of amyloid deposits. In: Kyle RA, Gertz MA, eds. *Amyloid and Amyloidosis, 1998*. Pearl River, NY: Parthenon Publishing; 1999:160–162.

18. Gilbertson JA, Hunt T, Hawkins PN. Amyloid typing: experience from a large referral centre. In: Picken M, Dogan A, Herrera G, eds. *Amyloid and Related Disorders. Current Clinical Pathology*. New York, NY: Humana Press; 2012:231–238.

19. Dasari S, Theis JD, Vrana JA, et al. Proteomic detection of immunoglobulin light chain variable region peptides from amyloidosis patient biopsies. *J Proteome Res*. 2015;14:1957–1967.

20. Sethi S, Dasari S, Plaisier E, et al. Apolipoprotein CII amyloidosis associated with p.Lys41Thr mutation. *Kidney Int Rep*. 2018;3:1193–1201.

21. Sethi S, Vrana JA, Theis JD, et al. Laser microdissection and mass spectrometry-based proteomics aids the diagnosis and typing of renal amyloidosis. *Kidney Int*. 2012;82: 226–234.

22. Vrana JA, Gamez JD, Madden BJ, et al. Classification of amyloidosis by laser microdissection and mass spectrometry-based proteomic analysis in clinical biopsy specimens. *Blood*. 2009;114:4957–4959.

23. Vrana JA, Theis JD, Dasari S, et al. Clinical diagnosis and typing of systemic amyloidosis in subcutaneous fat aspirates by mass spectrometry-based proteomics. *Haematologica*. 2014;99:1239–1247.

24. Rodriguez FJ, Gamez JD, Vrana JA, et al. Immunoglobulin derived depositions in the nervous system: novel mass spectrometry application for protein characterization in formalin-fixed tissues. *Lab Invest*. 2008;88:1024–1037.

25. Lavatelli F, Valentini V, Palladini G, et al. Mass spectrometry-based proteomics as a diagnostic tool when immunoelectron microscopy fails in typing amyloid deposits. *Amyloid*. 2011;18(suppl 1):64–66.

26. Gilbertson JA, Theis JD, Vrana JA, et al. A comparison of immunohistochemistry and mass spectrometry for determining the amyloid fibril protein from formalin-fixed biopsy tissue. *J Clin Pathol*. 2015;68:314–317.

27. Rezk T, Gilbertson JA, Mangione PP, et al. The complementary role of histology and proteomics for diagnosis and typing of systemic amyloidosis [e-pub ahead of print]. J Pathol Clin Res. https://doi.org/10.1002/cjp2.126, accessed April 15, 2019.

28. Rowczenio D, Stensland M, de Souza GA, et al. Renal amyloidosis associated with 5 novel variants in the fibrinogen A Alpha chain protein. *Kidney Int Rep*. 2017;2: 461–469.

29. Canetti D, Rendell NB, Di Vagno L, et al. Misidentification of transthyretin and immunoglobulin variants by proteomics due to methyl lysine formation in formalin-fixed paraffin-embedded amyloid tissue. *Amyloid*. 2017;24:233–241.

30. Mangione PP, Mazza G, Gilbertson JA, et al. Increasing the accuracy of proteomic typing by decellularisation of amyloid tissue biopsies. *J Proteomics*. 2017;165:113–118.

31. Talmud P, Tybjaerg-Hansen A, Bhatnagar D, et al. Rapid screening for specific mutations in patients with a clinical diagnosis of familial hypercholesterolaemia. *Atherosclerosis*. 1991;89:137–141.

32. Nasr SH, Dasari S, Mills JR, et al. Hereditary lysozyme amyloidosis variant p.Leu102Ser associates with unique phenotype. *J Am Soc Nephrol*. 2017;28:431–438.

33. Rezk T, Gilbertson JA, Rowczenio D, et al. Diagnosis, pathogenesis and outcome in leucocyte chemotactic factor 2 (ALECT2) amyloidosis. *Nephrol Dial Transplant*. 2018;33:241–247.

34. Aoki M, Kang D, Katayama A, et al. Optimal conditions and the advantages of using laser microdissection and liquid chromatography tandem mass spectrometry for diagnosing renal amyloidosis. *Clin Exp Nephrol*. 2018;22:871–880.

35. Jullig M, Browett P, Middleditch MM, et al. A unique case of neural amyloidoma diagnosed by mass spectrometry of formalin-fixed tissue using a novel preparative technique. *Amyloid*. 2011;18:147–155.

36. Shteynberg D, Nesvizhskii AI, Moritz RL, et al. Combining results of multiple search engines in proteomics. *Mol Cell Proteomics*. 2013;12:2383–2393.

37. Sidiqi MH, McPhail ED, Theis JD, et al. Two types of amyloidosis presenting in a single patient: a case series. *Blood Cancer J*. 2019;9:30.